

MICROCOPY RESOLUTION TEST CHART  
NATIONAL BUREAU OF STANDARDS-1963-A

AD-A154 387

**INVESTIGATION FOR LOW-COST  
PERMANENT MAGNETS**

**Final Report  
Contract No. N00014-80-C-0566**

**Prepared for**

**Department of the Navy  
Office of Naval Research  
Arlington, Virginia 22217**

**Prepared by**

**Alloy Properties Branch  
Metallurgy Laboratory  
Corporate Research and Development  
General Electric Company  
Schenectady, New York 12301**

**March 1985**

**DTIC  
ELECTE  
MAY 30 1985  
S A D**

**Reproduction in whole or in part is permitted for any  
purpose of the United States Government**

**Approved for public release: distribution unlimited.**

DTIC FILE COPY

unclassified

SECURITY CLASSIFICATION OF THIS PAGE

REPORT DOCUMENTATION PAGE

1a. REPORT SECURITY CLASSIFICATION <b>unclassified</b>		1b. RESTRICTIVE MARKINGS	
2a. SECURITY CLASSIFICATION AUTHORITY		3. DISTRIBUTION/AVAILABILITY OF REPORT <b>Approved for public release; distribution unlimited</b>	
2b. DECLASSIFICATION/DOWNGRADING SCHEDULE			
4. PERFORMING ORGANIZATION REPORT NUMBER(S) <b>85-SRD-013</b>		5. MONITORING ORGANIZATION REPORT NUMBER(S)	
6a. NAME OF PERFORMING ORGANIZATION <b>General Electric Company Corporate Research and Development</b>	8b. OFFICE SYMBOL <i>(If applicable)</i>	7a. NAME OF MONITORING ORGANIZATION	
6c. ADDRESS (City, State and ZIP Code) <b>Schenectady, NY 12301</b>		7b. ADDRESS (City, State and ZIP Code)	
8a. NAME OF FUNDING/SPONSORING ORGANIZATION <b>Department of the Navy Office of Naval Research</b>	8b. OFFICE SYMBOL <i>(If applicable)</i> <b>Code 430</b>	9. PROCUREMENT INSTRUMENT IDENTIFICATION NUMBER <b>N00014-80-C-0566</b>	
8c. ADDRESS (City, State and ZIP Code) <b>Arlington, VA 22217</b>		10. SOURCE OF FUNDING NOS.	
11. TITLE (Include Security Classification) <b>Investigation for Low-Cost Permanent Magnets unclassified</b>		PROGRAM ELEMENT NO.	PROJECT NO.
12. PERSONAL AUTHOR(S) <b>J.J. Becker</b>		TASK NO.	WORK UNIT NO.
13a. TYPE OF REPORT <b>Final Report</b>	13b. TIME COVERED <b>FROM July 1980 TO Dec 1983</b>	14. DATE OF REPORT (Yr., Mo., Day) <b>March 1985</b>	
15. PAGE COUNT <b>9</b>			
16. SUPPLEMENTARY NOTATION			
17. COSATI CODES		18. SUBJECT TERMS (Continue on reverse if necessary and identify by block number)	
FIELD	GROUP	SUB. GR.	
		<b>permanent magnets, magnetic materials, amorphous metals, crystallization</b>	
19. ABSTRACT (Continue on reverse if necessary and identify by block number)			
<p>This work focused on the search for materials and processing techniques that provide the potential of low-cost, high-performance permanent magnets. The principal processing method was rapid solidification and annealing. Crystallized amorphous alloys of Fe, Co, Ni, and glass formers exhibited coercivities of several hundred oersteds. A coercive force, <math>H_{ci}</math>, of 960 Oe was attained in <math>Fe_{25}V_{15}P_{10}B_{10}</math> and 3,200 Oe in <math>Cu_{15}Co_{60}Si_{15}B_{10}</math>. Alloys containing Pr or Nd with Fe and B exhibited very high <math>H_{ci}</math> (over 20,000 Oe). These alloys are particularly attractive because of their high coercivity and magnetization, the absence of Co, and the relatively low content of the abundant light rare earths.</p> <p><i>Additional key words: amorphous magnets</i></p>			
20. DISTRIBUTION/AVAILABILITY OF ABSTRACT UNCLASSIFIED/UNLIMITED <input type="checkbox"/> SAME AS RPT. <input checked="" type="checkbox"/> DTIC USERS <input type="checkbox"/>		21. ABSTRACT SECURITY CLASSIFICATION <b>unclassified</b>	
22a. NAME OF RESPONSIBLE INDIVIDUAL <b>D.E. Polk</b>		22b. TELEPHONE NUMBER <i>(Include Area Code)</i> <b>(202) 696-4402</b>	22c. OFFICE SYMBOL <b>Code 430</b>

## Section 1

### SUMMARY

The possibility of good permanent magnet properties is suggested by the coercive forces,  $H_{ci}$ , that sometimes appear when amorphous metals, initially magnetically soft, are annealed until crystallization occurs. This report describes the studies carried out in our laboratory in our search for low-cost, high-performance permanent magnets. In the first two years of the contract the focus was on alloys not containing rare earths. In the last 16 months, iron-based alloys containing light rare earths and metalloids were explored. Since the completion of this work several companies have begun production of iron-rare earth magnets based on their own independent work.

**Nonrare-earth alloys.** An initial survey of many crystallized amorphous alloys of Fe, Co, Ni, and various glass formers indicated that  $H_{ci}$  of several hundred oersteds could be attained in some compositions. Rapid annealing by brief current pulses through the sample was found to be convenient and sometimes led to higher  $H_{ci}$  than conventional annealing. In a number of instances, remanence ratios,  $M_r/M_s$ , of more than 0.8 were obtained in these materials; such values imply the presence of phases with higher magnetic symmetry than single-easy-axis.

Alloys have been made that contain Cr or V and are nonmagnetic when amorphous but strongly magnetic in the crystalline state.  $H_{ci}$  of 960 Oe was attained in  $\text{Fe}_{65}\text{V}_{15}\text{P}_{10}\text{B}_{10}$  that was treated by current-pulse annealing.

Alloys containing Cu were prepared in an attempt to obtain two-phase amorphous materials.  $H_{ci}$  of 3,200 Oe was attained in a pulse-annealed ribbon of  $\text{Cu}_{15}\text{Co}_{60}\text{Si}_{15}\text{B}_{10}$ , a value higher than that of any cobalt alloy not containing platinum or a rare earth.

**Alloys containing rare earths.** A large number of alloys based on iron, a light rare earth, and a glass former have been investigated. Prepared by rapid solidification at various rates, these materials exhibited very high  $H_{ci}$  (over 20,000 Oe) in  $\text{Fe}_{76}\text{Pr}_{16}\text{B}_5\text{Si}_3$ ,  $\text{Fe}_{76}\text{Nd}_{16}\text{B}_5\text{Si}_3$ , the same alloys with  $\text{B}_8$  instead of  $\text{B}_5\text{Si}_3$ , and in alloys with varying amounts of Fe and rare earth. These values were obtained in material as quenched on a rapidly rotating copper wheel without further treatment. Sm did not reach as high  $H_{ci}$  but showed very high  $M_r/M_s$ . These studies have shown that B is necessary for high  $H_{ci}$ , while neither Si nor C alone are effective.

Measurements of magnetization as a function of temperature indicated a Curie temperature,  $T_c$ , of about 310 °C for the high- $H_{ci}$  phase. The amorphous phase and a high- $T_c$   $\alpha$ -Fe phase were also identified. In optimum quench rate, the predominant phase was the 310 °C phase. The optimum material contained equiaxed grains about 500 nm in diameter which were identified by electron and X-ray diffraction as the intermetallic compound  $\text{Fe}_{14}\text{Pr}_2\text{B}_1$ . This high- $H_{ci}$  phase with  $T_c$  of 310 °C can also be produced by the annealing of initially amorphous material.

As-cast ingots showed the high- $H_{ci}$  phase, as indicated by X-ray diffraction and Curie temperature measurements. Samples were prepared by grinding ingot material to powder and aligning in a field. An alloy of  $\text{Fe}_{76}\text{Pr}_{16}\text{B}_8$  prepared in this way had  $H_{ci}$  of 3,600 Oe and  $M_r/M_s = 0.9$ . These experiments strongly suggest the possibility of preparing the high- $H_{ci}$  material directly without special rapid solidification procedures. Fabrication of magnets could be accomplished by conventional pressing and sintering processes.

**Section 2**  
**INTRODUCTION**

Amorphous magnetic alloys can have attractive soft magnetic properties, arising from their lack of macroscopic magnetic anisotropy. The coercive forces of alloys of the Fe-Ni-P-B type as prepared can be as low as 0.10 Oe.<sup>(1)\*</sup> Annealing at low temperatures can reduce  $H_c$  still further. A  $Fe_{40}Ni_{40}P_{14}B_6$  alloy annealed for 25 minutes at 330 °C had  $H_c < 0.003$  Oe.<sup>(2)</sup> As the annealing temperature is raised,  $H_c$  suddenly rises by several orders of magnitude, signifying the onset of crystallization.<sup>(3)</sup> The structure changes from a homogeneous glass to a fine dispersion of several phases, some of which may have high magnetocrystalline anisotropy. The rise in  $H_c$  on crystallization is so striking that it is natural to ask how far the permanent magnet properties of crystallized amorphous metals could be developed under the most favorable circumstances.

Permanent magnet materials are distinguished by microstructures including two magnetically different phases on an extremely fine scale, as in the Alnicos and Fe-Cr-Co alloys; high magnetocrystalline anisotropy, as in Co-Sm and the barium ferrites; or both, as in the Cu-modified cobalt-rare-earths and their descendants. These microstructures result from various processing and heat treatment procedures. Such structures can also be produced by crystallizing amorphous alloys, or directly by rapid quenching. These processes lead to fine-scale heterogeneity and can also result in the production of phases, for example  $Fe_3B$ ,<sup>(4)</sup> that would not be stable under more nearly equilibrium conditions. Such phases may have low symmetry and possibly high magnetocrystalline anisotropy. For all these reasons crystallized amorphous materials seemed attractive to explore for potential permanent magnet properties.

Accession For	
NTIS GRAM	<input checked="" type="checkbox"/>
DTIC TAB	<input type="checkbox"/>
Unannounced	<input type="checkbox"/>
Justification	
By _____	
Distribution/	
Availability Codes	
Dist	Avail and/or Special
A-1	

\* References are given in Section 7.



### Section 3

## PREVIOUS STUDIES

There have been many studies of the morphology and kinetics of crystallization in a variety of amorphous alloys, utilizing microscopy, diffraction, calorimetry, resistance measurements, and other techniques.<sup>(5)</sup> However, magnetic effects resulting from crystallization have received relatively little attention. Measurements of magnetization as a function of temperature characteristically show magnetization decreasing with increasing temperature as the  $T_c$  of the amorphous phase is approached, then rising again as crystalline material with higher  $T_c$  is formed during the course of the experiment.<sup>(6)</sup>

There have been a few studies of the effect of crystallization on the magnetic hysteresis behavior. As mentioned above,  $H_c$  has been used as an indication of the beginning of crystallization in stability studies.<sup>(3)</sup> The coercive forces obtained during various crystallization anneals have been studied by Takahashi, Miyazaki, Ono, and Takakura,<sup>(7)</sup> who prepared amorphous alloys of  $\text{Fe}_{80}\text{P}_{13}\text{C}_7$  with  $H_c$  much less than 1 Oe. Upon annealing, the room temperature  $H_c$  abruptly increased at 400 °C, reached a maximum of 150 Oe for a 420 °C anneal, and decreased again with higher annealing temperatures. The broad amorphous X-ray peaks of the initial material disappeared at 400 °C, to be replaced by lines of  $\alpha$ -Fe and  $\text{Fe}_3\text{P}$ , and at higher temperatures also  $\text{Fe}_3\text{B}$ .

Coercive force versus annealing temperature curves for the alloy  $\text{Fe}_5\text{Co}_{70}\text{Si}_{15}\text{B}_{10}$  have been reported.<sup>(8)</sup> Again,  $H_c$  rises sharply with annealing temperatures around 400 °C, reaches a maximum (in this case, 300 Oe) at 500 °C, and decreases with higher annealing temperature. The high  $H_c$  was attributed to finely dispersed cubic cobalt.

Amorphous alloys around the composition  $\text{Fe}_{80}(\text{B,C,Si})_{20}$  have good soft properties. Their crystallization begins with the formation of  $\alpha$ -Fe dendrites. The dependence of  $H_c$  on dendrite dimensions and number density has been studied.<sup>(9,10)</sup>

Ramanan, Martin, and Macur<sup>(11)</sup> studied the increase in  $H_c$  brought about by a small amount of eutectic crystallization in  $\text{Fe}_{77}\text{B}_{23}$ .

Bhatti, Grundy, Jones, Scarsbrook, and Tebble<sup>(12)</sup> have reported observations by Lorentz electron microscopy of the pinning of domain boundaries by  $\text{Fe}_3\text{B}$  spherulites in an amorphous Fe-B matrix.

## Section 4

### NONRARE-EARTH ALLOYS

#### A. Composition

An initial exploratory survey<sup>(13)</sup> indicated that crystallized amorphous alloys of Fe, Ni, and various glass formers tended to develop higher intrinsic coercive force,  $H_{ci}$ , when C and P were present rather than B. This is consistent with the variation of the easy-axis anisotropy of  $\text{Fe}_3(\text{B,P,C})$  with composition.

In  $(\text{Fe,Ni})_{80}\text{P}_{20}$  there is a sudden drastic decrease in  $H_{ci}$  as the composition goes from  $\text{Fe}_{40}\text{Ni}_{40}\text{P}_{20}$  to  $\text{Fe}_{50}\text{Ni}_{30}\text{P}_{20}$ . This is associated with the appearance of a soft BCC  $\alpha$ -Fe phase.

#### B. Current Pulse Annealing

A technique used in these investigations in addition to conventional furnace annealing was the rapid heating of the material for very short times by the passage of electrical current pulses through the sample.<sup>(14)</sup> This often resulted in  $H_{ci}$  higher than the best that could be attained by furnace annealing, probably because the much higher heating rate produced a finer structure and perhaps suppressed low-temperature phases. In this way an  $H_{ci}$  of 420 Oe was attained in  $\text{Fe}_{40}\text{Ni}_{40}\text{P}_{20}$ , and a value of 830 Oe in  $\text{Fe}_5\text{Co}_{70}\text{Si}_{15}\text{B}_{10}$ , far higher than the values reported<sup>(8)</sup> for isothermal anneals of the same alloy.

#### C. Remanence Ratios

In a number of instances  $M_r/M_s$  ratios of more than 0.8 have been obtained, implying the presence of phases with higher symmetry than single-easy-axis. For randomly oriented particles,  $M_r/M_s$  can vary from 0.5 for easy-axis particles to 0.87 for cube-diagonal easy directions, for any measurement direction. We measured 0.82 in  $\text{Fe}_5\text{Co}_{70}\text{Si}_{15}\text{B}_{10}$ , consistent with the observation that high  $H_{ci}$  is associated with the presence of FCC cobalt.

#### D. Partial Crystallization of Initially Nonmagnetic Amorphous Phases

It is possible to make iron-rich alloys that are nonferromagnetic at room temperature in the amorphous state but strongly ferromagnetic when crystalline. This can be done by the replacement of around 20% of the Fe by Cr, V, Mn, and probably other transition elements. Alloys containing Cr and V have been prepared. With 10 to 20% Cr or V, the Curie temperatures of the amorphous phases are in the vicinity of room temperature.<sup>(15)</sup> When these alloys are partially crystallized,  $H_{ci}$  can be observed to increase several times over with increasing temperature as the matrix becomes nonmagnetic. The highest room-temperature  $H_{ci}$  attained in this type of alloy was 960 Oe in  $\text{Fe}_{65}\text{V}_{15}\text{P}_{10}\text{B}_{10}$ , treated by current-pulse annealing.

#### E. Two-phase Amorphous Alloys

Many ordinary glasses are two-phase, often forming a very fine, compositionally modulated structure by decomposing in spinodal fashion. Metallic glasses can also show two amorphous phases,<sup>(16-18)</sup> sometimes with extremely fine microstructures. Various Fe-Co-B-Si alloys were modified by the addition of 5 to 20% Cu, hoping that phase separation would occur in the quenched ribbons, because Cu-Fe and Cu-Co are on the verge of liquid immiscibility. We obtained an intrinsic coercive force of 3200 Oe in a pulse-annealed ribbon of  $\text{Cu}_{15}\text{Co}_{60}\text{Si}_{15}\text{B}_{10}$ , which is higher than that of any cobalt alloy not containing platinum or a rare earth.

## Section 5

### ALLOYS CONTAINING RARE EARTHS

The highest coercive forces and energy products among commercial permanent magnet materials are found in the cobalt-rare earths. The high  $H_{ci}$  result from the very high magnetocrystalline anisotropy that can occur in intermetallic compounds containing transition metals and rare earths.

Rapidly quenched metals containing rare earths can also show high  $H_{ci}$ , either as quenched or after subsequent annealing. Sputtered films of  $\text{Fe}_2\text{Tb}$ ,  $\text{Fe}_2\text{Dy}$ , and  $\text{Fe}_2\text{Sm}$  have been shown to have  $H_{ci}$  in the range of 30 kOe at 4.2 K,<sup>(19)</sup> although their room-temperature  $H_{ci}$  are low. A film of  $\text{Fe}_2\text{Tb}$ , with an initial room-temperature  $H_{ci}$  of 120 Oe, was annealed at various temperatures with the result that the room-temperature  $H_{ci}$  suddenly increased to 3500 Oe as the annealing temperature reached 300 to 350 °C. This was accompanied by an increase in magnetization to that of crystalline material.

Melt-spun alloys containing rare earths show remarkable behavior. Koon and Das<sup>(20)</sup> found that they could add several percent of Tb to conventionally melt-spun Fe-B alloys if they also added a small amount of La, which apparently inhibits the crystallization of rare-earth phases. The alloys were originally prepared so that their magnetostrictive properties might be investigated. They were magnetically soft as spun, but on annealing at temperatures around 650 °C the alloys developed  $H_{ci}$  of several thousand oersteds. The remanence of  $\text{Fe}_{73.8}\text{B}_{16.2}\text{Tb}_5\text{La}_5$  alloy was about 5000 G, with a pronounced dip in the second quadrant of the hysteresis loop. This loop shape and the low remanence would make such a material unfavorable for eventual use as a permanent magnet material. Becker<sup>(21)</sup> found a similar dip in  $\text{Fe}_{70.5}\text{B}_{15.5}\text{Tb}_7\text{La}_7$  and found that it could be removed by etching the ribbon, indicating that it was due to soft material at the surface. Electrical current pulse heating produced  $H_{ci}$  of almost 17 kOe in ribbons of this composition.

Croat and his coworkers have published a number of papers describing the properties of rapidly solidified alloys of Fe with Nd, Pr, and other rare earths.<sup>(22)</sup> These alloys contained only iron and rare earth, with no glass-forming elements. They were usually of a composition around  $\text{Fe}_{0.6}\text{R}_{0.4}$ . Room temperature  $H_{ci}$  was studied as a function of wheel speed in the melt-spinning apparatus. Maxima in  $H_{ci}$  of the as-spun material were found for wheel surface speeds in the range of 5-15 m/s. X-ray spectra seem to indicate that the optimum quenching rate produces a structure that is partially amorphous and partially crystalline.

Again, the hysteresis loops of these materials show low remanences and unfavorable second quadrant shapes, leading to reported maximum energy products in the range of 3-4 MGOe.

Hadjipanayis, Hazelton, Lawless, and Sellmyer<sup>(23)</sup> prepared rapidly quenched Fe-Tb alloys with some of the Tb replaced by light rare earths and attained  $H_{ci}$  of several kilo-oersteds in  $\text{Fe}_2\text{PrTb}$ , although with low magnetization. More recently, Hadjipanayis, Hazelton, and Lawless<sup>(24)</sup> have investigated Fe-Pr-B-Si alloys and have obtained values of  $B_r = 7500$  G,  $H_{ci} = 15$  kOe, and  $(\text{BH})_m = 12$  MGOe in an alloy of composition  $\text{Fe}_{76}\text{Pr}_{16}\text{B}_5\text{Si}_3$  rapidly quenched and then heat treated at 750 °C. They attributed the good properties to the presence of a tetragonal  $\text{Fe}_{20}\text{R}_3\text{B}$  phase isostructural with  $\text{Fe}_{20}\text{G}_3\text{C}_{25}$  with  $a = 8.8$  Å and  $c = 11.8$  Å.

We have investigated a number of alloys of compositions based on that first reported by Hadjipanayis, Hazelton, and Lawless.<sup>(24)</sup> The results of our work have been documented in three publications which appear as appendixes to this report.

## Section 6

### CONTRACT PUBLICATIONS

Work on this contract since its initiation in July 1980 has resulted in five publications in the scientific literature:

1. "Surface Effects on Hysteresis Loop Shapes in High-Coercive-Force Crystallized Amorphous Alloys," J.J. Becker, *IEEE Trans. Magn. MAG-18*, 1451 (1982).
2. "Composition Dependence of Coercive Force of Some Crystallized Amorphous Alloys," J.J. Becker, *IEEE Trans. Magn. MAG-19*, 2033 (1983).
3. "Rapidly Quenched Metals for Permanent Magnet Materials," J.J. Becker, *J. of Applied Physics* 55, 2067 (1984). Appendix A of this report.
4. "Thermal Effects of Moderate Substitutions of Cobalt for Iron in  $\text{Fe}_{76}\text{Pr}_{16}\text{B}_8$ ," R.A. Overfelt and J.J. Becker, *Applied Physics Letters* 44, 925 (1984). Appendix B of this report.
5. "Surface Effects on the Coercive Force of Rapidly Solidified Fe-Pr-B Alloys," J.J. Becker and R.A. Overfelt, *IEEE Trans. Magn. MAG-20*, 1596 (1984). Appendix C of this report.

Section 7  
REFERENCES

1. T. Egami, P.J. Flanders, and C.D. Graham, Jr., *AIP Conf. Proc.* 24, 697 (1975).
2. F.E. Luborsky, J.J. Becker, and R.O. McCary, *IEEE Trans. MAG-11*, 1644 (1975).
3. F.E. Luborsky, *Mat. Sci. and Eng.* 28, 139 (1977)
4. R. Hasegawa, R.C. O'Handley, and L.I. Mendelsohn, *AIP Conf. Proc.* 34, 298 (1976).
5. U. Koster and U. Herold, *Glassy Metals*, H.J. Guntherodt and H. Beck, ed., p. 225, Springer-Verlag, Heidelberg (1981).
6. M. Takahashi and M. Koshimura, *Japan. J. Appl. Phys.* 16, 1771, 2269 (1977); M. Takahashi, C.O. Kim, M. Koshimura, and T. Suzuki, *Japan. J. Appl. Phys.* 17, 1911 (1978).
7. M. Takahashi, T. Miyazaki, F. Ono, and K. Takakura, *J. Japan Inst. Metals* 40, 1192 (1976).
8. A.A. Glazer, A.P. Potapov, V.V. Serikov, R.I. Tagirov, Y.I. Teytel, G.M. Makarova, and N.M. Kleynerman, *Fiz. met. metalloved.* 48, 1165 (1979); *Phys. Met. Metall.* 48, 33 (1979).
9. J.C. Swartz, J.J. Haugh, R.F. Krause, and R. Kossowski, *J. Appl. Phys.* 52, 1908 (1981).
10. S.F.H. Parker, P.J. Grundy, G.A. Jones, and R.S. Tebble, *J. Appl. Phys.* 53, 7840 (1982).
11. V.R.V. Ramanan, J. Marti, and J. Macur, *J. Appl. Phys.* 52, 1874 (1981).
12. A.R. Bhatti, P.J. Grundy, G.A. Jones, D.A. Scarsbrook, and R.S. Tebble, *IEEE Trans. MAG-16*, 1437 (1980).
13. J.J. Becker, IEEE Intermag Conference, April 5-8, 1983; to be published, *IEEE Trans. on Magnetics*.
14. T. Jagielinski, IEEE Intermag Conference, April 5-8, 1983; to be published, *IEEE Trans. on Magnetics*.
15. T. Mizoguchi, K. Yamauchi, and H. Miyajima, *Proc. Intern. Conf. on Magnetism, Vol II*, Moscow, August 1973; Nauka, Moscow (1974).
16. C.P. Chou and D. Turnbull, *J. Non-Cryst. Solids* 17, 169 (1975).
17. L.E. Tanner and R. Ray, *Scripta Met.* 14, 657 (1980).
18. J.L. Walter, S.F. Bartram, and I. Mella, *Mat. Sci. and Eng.* 36, 193 (1978).
19. A.E. Clark, *Appl. Phys. Lett.* 23, 642 (1973).
20. N.C. Koon and B.N. Das, *Appl. Phys. Lett.* 39, 840 (1981).
21. J.J. Becker, *IEEE Trans. MAG-18*, 1451 (1982).

22. J.J. Croat, *IEEE Trans. MAG-18*, 1442 (1982).
23. G.C. Hadjipanayis, R.C. Hazelton, K. Lawless, and D.J. Sellmyer, *J. Magn. Magn. Mater.* 40, 278 (1984).
24. G.C. Hadjipanayis, R.C. Hazelton, and K.R. Lawless, *Appl. Phys. Lett.*, 43, 797 (1983).
25. H.H. Stadelmaier and H.K. Park, *Z. Metallk.* 72, 417 (1981).

**APPENDIX A**  
**84CRD094**

# CRD

---

Corporate Research and Development

---

Schenectady, New York

---

**RAPIDLY QUENCHED METALS  
FOR PERMANENT MAGNET MATERIALS**

by

**J. J. Becker  
Metallurgy Laboratory**

**Report No. 84CRD094**

**May 1984**

---

Technical Information Series

---

Class 1

---

**GENERAL  ELECTRIC**

# TECHNICAL INFORMATION SERIES

<b>AUTHOR</b> Becker, J J	<b>SUBJECT</b> permanent magnetic materials	<b>NO.</b> 84CRD094
		<b>DATE</b> May 1984
<b>TITLE</b> Rapidly Quenched Metals for Permanent Magnet Materials		<b>GE CLASS</b> 1
		<b>NO. PAGES</b> 8
<b>ORIGINATING COMPONENT</b> Metallurgy Laboratory		<b>CORPORATE RESEARCH AND DEVELOPMENT</b> SCHENECTADY, N.Y.
<b>SUMMARY</b>  When magnetically soft amorphous metals are annealed until crystallization occurs, coercive forces sometimes arise that are high enough to suggest the possibility of permanent magnet materials. This paper begins with a brief review of results in alloys not containing rare earths. Then earlier results on rare-earth-modified Fe-B alloys and on Fe-R alloys quenched at intermediate rates are reviewed. Recent experiments indicate that intrinsic coercive forces of many kOe combined with high $M_s$ and $M_r$ are possible in rapidly quenched alloys containing only iron, light rare earths, and glass formers. Recent work and our current results in these alloys are presented and discussed, including effects of composition, quenching rate, annealing, and etching, as well as thermomagnetic effects and phase identification.		
<b>KEY WORDS</b> permanent magnet, magnetic materials, rapid solidification, Curie temperature		

**INFORMATION PREPARED FOR** \_\_\_\_\_  
\_\_\_\_\_

**Additional Hard or Microfiche Copies Available from**

**Technical Information Exchange  
Bldg. 5 Room 321, Schenectady, N.Y. 12345**

# RAPIDLY QUENCHED METALS FOR PERMANENT MAGNET MATERIALS

J. J. Becker

## INTRODUCTION

Amorphous magnetic alloys can have attractive soft magnetic properties, arising from their lack of macroscopic magnetic anisotropy. The coercive forces of alloys of the Fe-Ni-P-B type as prepared can be as low as 0.10 Oe.<sup>1</sup> Annealing at low temperatures can reduce  $H_c$  still further. A  $Fe_{40}Ni_{40}P_{14}B_6$  alloy annealed for 25 minutes at 330°C had  $H_c < 0.003$  Oe.<sup>2</sup> As the annealing temperature is raised,  $H_c$  suddenly rises by several orders of magnitude, signifying the onset of crystallization.<sup>3</sup> The structure is changing from a homogeneous glass to a fine dispersion of several phases, some of which may have high magnetocrystalline anisotropy. The rise in  $H_c$  on crystallization is so striking that it is natural to ask how far the permanent magnet properties of crystallized amorphous metals could be developed under the most favorable circumstances.

Permanent magnet materials are distinguished by microstructures including two magnetically different phases on an extremely fine scale, as in the Alnicos and Fe-Cr-Co alloys, high magnetocrystalline anisotropy, as in Co-Sm and the barium ferrites, or both, as in the Cu-modified cobalt-rare-earths and their descendants. These microstructures result from various processing and heat treatment procedures. Such structures can also be produced by crystallizing amorphous alloys or directly by rapid quenching. These processes lead to fine-scale heterogeneity and can also result in the production of phases, for example  $Fe_3B$ ,<sup>4</sup> that would not be stable under more nearly equilibrium conditions. Such phases may have low symmetry and possibly high magnetocrystalline anisotropy. For all these reasons crystallized amorphous materials seemed attractive to explore for potential permanent magnet properties.

## PREVIOUS STUDIES

There have been many studies of the morphology and kinetics of crystallization in a variety of amorphous alloys, utilizing microscopy, diffraction,

calorimetry, resistance measurements, and other techniques.<sup>5</sup> However, magnetic effects resulting from crystallization have received relatively little attention. Measurements of magnetization as a function of temperature characteristically show  $M$  decreasing with increasing  $T$  as the  $T_c$  of the amorphous phase is approached, then rising again as crystalline material with higher  $T_c$  is formed during the course of the experiment.<sup>6</sup>

There have been a few studies of the effect of crystallization on the magnetic hysteresis behavior. As mentioned above,  $H_c$  has been used as an indication of the beginning of crystallization in stability studies.<sup>3</sup> The coercive forces obtained during various crystallization anneals have been studied by Takahashi, Miyazaki, Ono, and Takakura,<sup>7</sup> who prepared amorphous alloys of  $Fe_{80}P_{13}C_7$  whose  $H_c$  was much less than one Oe. Upon annealing, the room temperature  $H_c$  abruptly increased at 400°C, reached a maximum of 150 Oe for a 420°C anneal, and decreased again with higher annealing temperatures. The broad amorphous X-ray peaks of the initial material disappeared at 400°C, to be replaced by lines of  $\alpha$ -Fe and  $Fe_3P$ , then at higher temperatures also  $Fe_3B$ .

Coercive force versus annealing temperature curves for the alloy  $Fe_5Co_{70}Si_{15}B_{10}$  have been reported.<sup>8</sup> Again  $H_c$  rises sharply with annealing temperatures around 400°C, reaches a maximum, in this case 300 Oe, at 500°C, and decreases with higher annealing temperature. The high  $H_c$  was attributed to finely dispersed cubic cobalt.

Amorphous alloys around the composition  $Fe_{80}(B,C,Si)_{20}$  have good soft properties. Their crystallization begins with the formation of  $\alpha$ -Fe dendrites. The dependence of  $H_c$  on dendrite dimensions and number density has been studied.<sup>9,10</sup>

Ramanan, Martin and Macur<sup>11</sup> studied the increase in  $H_c$  brought about by a small amount of eutectic crystallization in  $Fe_{77}B_{23}$ .

Bhatti, Grundy, Jones, Scarsbrook, and Tebble<sup>12</sup> have reported observations of Lorentz electron microscopy of the pinning of domain boundaries by Fe<sub>3</sub>B spherulites in an amorphous Fe-B matrix.

## NON-RARE-EARTH ALLOYS

### Composition

An initial exploratory survey<sup>13</sup> indicated that crystallized amorphous alloys of Fe, Ni, and various glass formers tended to develop higher intrinsic coercive force  $H_{ci}$  when C and P were present rather than B. This is consistent with the variation of the easy-axis anisotropy of Fe<sub>3</sub>(B,P,C) with composition.

In (Fe,Ni)<sub>80</sub>P<sub>20</sub> there is a sudden drastic decrease in  $H_{ci}$  as the composition goes from Fe<sub>40</sub>Ni<sub>40</sub>P<sub>20</sub> to Fe<sub>50</sub>Ni<sub>30</sub>P<sub>20</sub>. This is associated with the appearance of a soft BCC  $\alpha$ -Fe phase.

### Current pulse annealing

A technique used in these investigations in addition to conventional furnace annealing was the rapid heating of the material for very short times by the passage of electrical current pulses through the sample.<sup>14</sup> This often resulted in  $H_{ci}$  higher than the best that could be attained by furnace annealing, probably because the much higher heating rate produced a finer structure and perhaps suppressed low-temperature phases. In this way an  $H_{ci}$  of 420 Oe was attained in Fe<sub>40</sub>Ni<sub>40</sub>P<sub>20</sub>, and a value of 830 Oe in Fe<sub>5</sub>Co<sub>70</sub>Si<sub>15</sub>B<sub>10</sub>, far higher than the values reported<sup>8</sup> for isothermal anneals of the same alloy.

### Remanence ratios

In a number of instances we have obtained  $M_r/M_s$  ratios of more than 0.8, implying the presence of phases with higher symmetry than single-easy-axis. For randomly oriented particles,  $M_r/M_s$  can vary from 0.5 for easy-axis particles to 0.87 for cube-diagonal easy directions, for any measurement direction. We measured 0.82 in Fe<sub>5</sub>Co<sub>70</sub>Si<sub>15</sub>B<sub>10</sub>, consistent with the observation that high  $H_{ci}$  is associated with the presence of FCC cobalt.

### Partial crystallization of initially non-magnetic amorphous phases

It is possible to make iron-rich alloys that are non-ferromagnetic at room temperature in the amorphous

state but strongly ferromagnetic when crystalline. This can be done by the replacement of around 20% of the Fe by Cr, V, Mn, and probably other transition elements. Alloys containing Cr and V have been prepared. With 10 to 20% Cr or V, the Curie temperatures of the amorphous phases are in the vicinity of room temperature.<sup>15</sup> When these alloys are partially crystallized,  $H_{ci}$  can be observed to increase several times over with *increasing* temperature as the matrix goes non-magnetic. The highest room-T  $H_{ci}$  attained in this type of alloy was 960 Oe in Fe<sub>65</sub>V<sub>15</sub>P<sub>10</sub>B<sub>10</sub>, treated by current-pulse annealing.

### Two-phase amorphous alloys

Many ordinary glasses are two-phase, often forming a very fine compositionally modulated structure by decomposing in spinodal fashion. Metallic glasses can also show two amorphous phases,<sup>16-18</sup> sometimes with extremely fine microstructures. We modified various Fe-Co-B-Si alloys by the addition of 5 to 20% Cu, hoping that phase separation would tend to occur in the quenched ribbons, since Cu-Fe and Cu-Co are on the verge of liquid immiscibility. We attained an intrinsic coercive force of 3200 Oe in a pulse-annealed ribbon of Cu<sub>15</sub>Co<sub>60</sub>Si<sub>15</sub>B<sub>10</sub>, which is higher than that of any cobalt alloy not containing platinum or a rare earth.

## ALLOYS CONTAINING RARE EARTHS

The highest coercive forces and energy products among commercial permanent magnet materials are found in the cobalt-rare-earths. The high  $H_{ci}$  result from the very high magnetocrystalline anisotropy that can occur in intermetallic compounds containing transition metals and rare earths.

Rapidly quenched metals containing rare earths can also show high  $H_{ci}$ , either as quenched or after subsequent annealing. Sputtered films of Fe<sub>2</sub>Tb, Fe<sub>2</sub>Dy, and Fe<sub>2</sub>Sm have been shown to have  $H_{ci}$  in the range of 30 kOe at 4.2 K,<sup>19</sup> although their room-T  $H_{ci}$  are low. A film of Fe<sub>2</sub>Tb, with an initial room-T  $H_{ci}$  of 120 Oe, was annealed at various temperatures with the result that the room-T  $H_{ci}$  suddenly increased to 3500 Oe as the annealing temperature reached 300 to 350°C. This was accompanied by an increase in magnetization to that of crystalline material.

Melt-spun alloys containing rare earths also show remarkable behavior. Koon and Das<sup>20</sup> found that they could add several percent of Tb to conventionally melt-spun Fe-B alloys if they also added a small amount of La, which apparently inhibits the crystallization of rare-earth phases. The alloys were

originally prepared so that their magnetostrictive properties might be investigated. They were magnetically soft as spun, but on annealing at temperatures around 650°C the alloys developed  $H_{ci}$  of several thousand Oe. The remanence of a  $Fe_{73.8}B_{16.2}Tb_5La_5$  alloy was about 5000 G, with a pronounced dip in the second quadrant of the hysteresis loop. This loop shape, and the low remanence, would make such a material unfavorable for eventual use as a permanent magnet material. Becker<sup>21</sup> found a similar dip in  $Fe_{70.5}B_{15.5}Tb_7La_7$  and found that it could be removed by etching the ribbon, indicating that it was due to soft material at the surface. Electrical current pulse heating produced  $H_{ci}$  of almost 17 kOe in ribbons of this composition.

### Rapidly solidified iron-rare-earth alloys

Croat and his coworkers have published a number of papers describing the properties of rapidly solidified alloys of Fe with Nd, Pr, and other rare earths.<sup>22</sup> These alloys contained only iron and rare earth, with no glass-forming elements. They were usually of a composition around  $Fe_{0.6}R_{0.4}$ . Room temperature  $H_{ci}$  was studied as a function of wheel speed in the melt-spinning apparatus. Maxima in  $H_{ci}$  of the as-spun material were found for wheel surface speeds in the range of 5-15 m/s. X-ray spectra seem to indicate that the optimum quenching rate produces a structure that is partially amorphous and partially crystalline.

Again, the hysteresis loops of these materials show low remanences and unfavorable second quadrant shapes, leading to reported maximum energy products in the range of 3-4 MGOe.

Hadjipanayis, Hazelton, Lawless, and Sellmyer<sup>23</sup> prepared rapidly quenched Fe-Tb alloys with some of the Tb replaced by light rare earths and attained  $H_{ci}$  of several kOe in  $Fe_2PrTb$ , although with low magnetization. More recently<sup>24</sup> Hadjipanayis, Hazelton, and Lawless have investigated Fe-Pr-B-Si alloys and have obtained values of  $B_r = 7500$  G,  $H_{ci} = 15$  kOe, and  $(BH)_m = 12$  MGOe in an alloy of composition  $Fe_{76}Pr_{16}B_5Si_3$  rapidly quenched and then heat treated at 750°C. They attributed the good properties to the presence of a tetragonal  $Fe_{20}R_3B$  phase isostructural with  $Fe_{20}Gd_3C_{25}$  with  $a = 8.8$  Å and  $c = 11.8$  Å.

### EXPERIMENTS ON Fe-R-Si-B ALLOYS

We have investigated a number of alloys of compositions based on that first reported by

Hadjipanayis, Hazelton, and Lawless.<sup>24</sup> This work has been done in collaboration with R. A. Overfelt, who made most of the experimental measurements described below.

### Experimental

The alloys were RF melted in silica crucibles having 0.020" or 0.050" orifices. The molten alloy was ejected by argon pressure of about 20 psi on to a rotating copper wheel from a distance of about 1/2". The runs were made in an atmosphere of argon.

Magnetic hysteresis loops were measured in a vibrating-sample magnetometer. Magnetization versus temperature runs were done either in the VSM or in a Perkin-Elmer thermogravimetric apparatus modified as a Faraday balance.

### Effect of quenching rate

Figure 1 shows the intrinsic coercive force as a function of wheel speed for  $Fe_{76}R_{16}B_5Si_3$  for  $R = Pr, Nd, \text{ and } Sm$ . In each instance  $H_{ci}$  is low for the slowest and fastest speeds and is a maximum at an intermediate rate, as Croat found for alloys not containing glass formers. Each point in the figure represents an average of three or more samples.

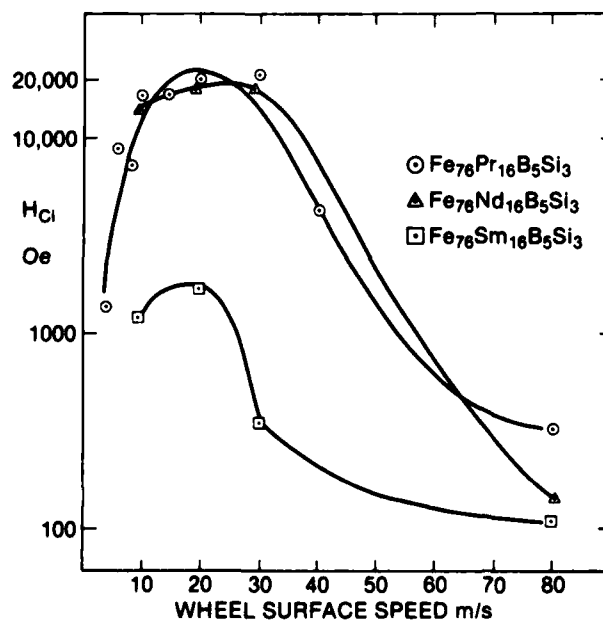


Figure 1.  $H_{ci}$  as a function of wheel surface speed in melt-spun alloys with three different rare earths.

The measurement of the coercive force was always done after the sample had been cooled from about 400°C in a field of 5000 Oe, after a magnetization-temperature run. In many cases this resulted in a displaced hysteresis loop, as in Figure 2, when the measurement was made in  $\pm 20$  kOe. Cooling in a field of the opposite polarity produced a loop of the opposite asymmetry, as in Figure 2. These are simply minor loops, since  $\pm 20$  kOe is not enough to saturate the material if  $H_{ci}$  is more than a few kOe. However, raising the temperature allows the material to be saturated even by a small field. Hysteresis loops measured at temperature became symmetrical as the temperature was raised. Cooling in a field is equivalent to applying a very large field at room temperature. The dip in magnetization at remanence is very characteristic<sup>20</sup> and generally indicates a soft surface layer that can be removed by etching.<sup>21</sup>

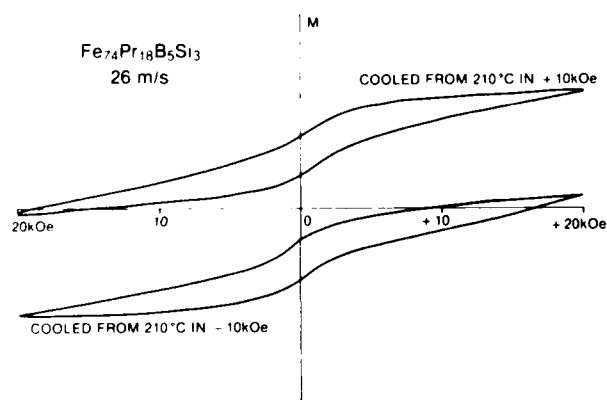


Figure 2. Displaced hysteresis loops resulting from cooling in a field of 10 kOe.

#### Effect of rare-earth composition

While Pr and Nd show similar behavior in Figure 1, Sm does not reach as high  $H_{ci}$ . However, unlike the others, it showed very high remanence. The  $M_r/M_s$  ratio was as high as 0.85 in some samples, in all directions. This implies higher than uniaxial symmetry, and, with the lower  $H_{ci}$ , suggests that the anisotropy of the hard phase in the Sm alloys is different from that in Pr and Nd.

#### Effect of glass-former composition

While B and Si were originally included in the alloys as glass formers, it appears that boron is neces-

sary to develop the high- $H_{ci}$  component of these materials. Figure 3 shows  $H_{ci}$  versus wheel speed for a series of alloys containing 76% Fe, 16% Pr, and 8% of various glass formers. Neither Si alone nor C alone give any indication of high  $H_{ci}$  in these experiments. Figure 4 shows various Fe-Pr-B compositions and again illustrates that without B these Fe-rich alloys do not develop high  $H_{ci}$ .

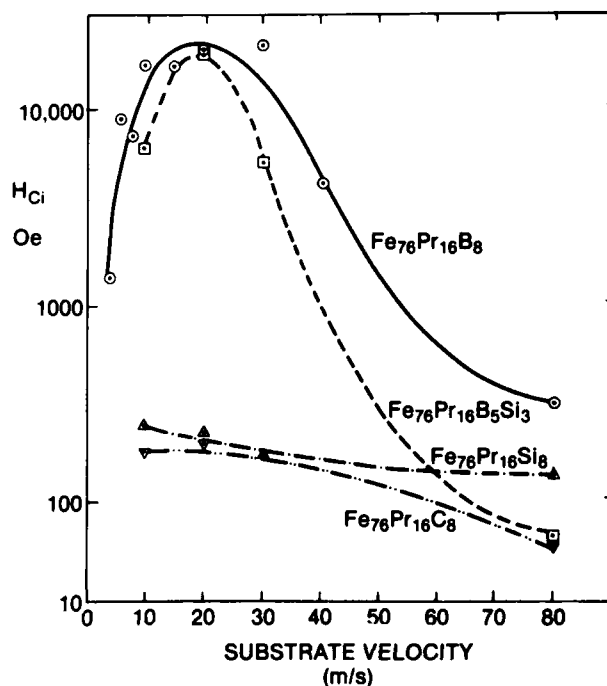


Figure 3.  $H_{ci}$  as a function of wheel surface speed in melt-spun alloys with different glass-formers.

#### Thermomagnetic measurements

Magnetization versus temperature curves were drawn using the vibrating-sample magnetometer with the sample inside a furnace consisting of a quartz tube with a tin oxide coating on its outside. The furnace could be heated by passing a current through the coating. Magnetization was recorded while the temperature was raised at approximately 50°C/min to about 400°C. This was done while the sample was in a constant field of 5000 Oe, following an initial magnetization in 20 kOe. Then the sample was cooled back to room temperature in the 5000 Oe field. After that the room-T hysteresis loop was drawn.

Three magnetic components could be seen in the magnetization-temperature curves. In the most rapidly solidified alloys, a  $T_c$  of about 160°C could

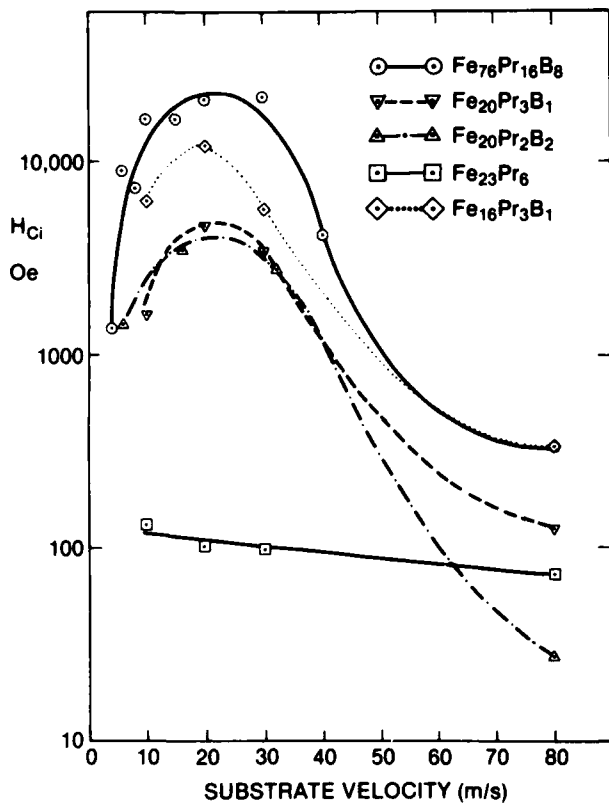


Figure 4.  $H_{ci}$  as a function of wheel surface speed in melt-spun alloys with varying amounts of boron.

be identified. In the alloys with the highest  $H_{ci}$ , there was a considerable amount of a material with  $T_c$  of about  $310^\circ\text{C}$ . Usually there was some quantity of a third phase whose magnetization remained quite constant up to  $400^\circ\text{C}$ . The first component is the amorphous phase, the second the high- $H_{ci}$  component, and the third a high- $T_c$   $\alpha$ -Fe-like phase. They will be referred to as amorphous, hard, and  $\alpha$ . An example of a thermomagnetic run that shows all three is seen in Figure 5. The figure shows how relative amounts and Curie temperatures were estimated. "Amount" here means specific magnetization (in 5000 Oe at room T) times quantity of material. The Curie temperature was taken as the point where the M-T curve began to become concave upward.

#### Dependence of properties on relative amounts of phases present

Figure 6 shows the relative amount of the three phases as a function of solidification rate for  $\text{Fe}_{76}\text{Pr}_{16}\text{B}_8$ . At high speeds, considerable amorphous

material forms and lowers  $H_{ci}$  because of its magnetic softness. On the other hand, the low  $H_{ci}$  at very slow speeds is not accompanied by a large increase in the amount of  $\alpha$  on any of these alloys, so it would appear to be due to the structure being too coarse.

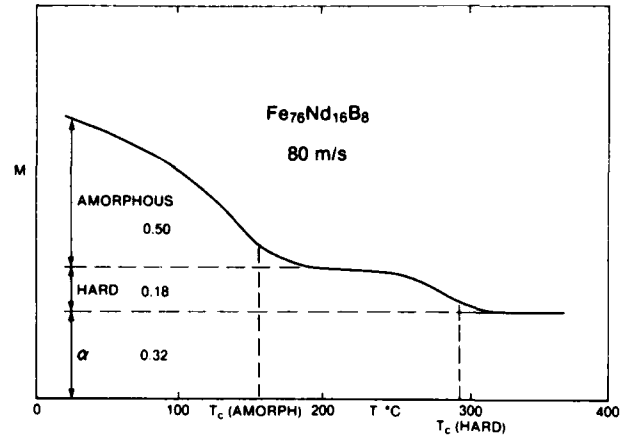


Figure 5. Magnetization versus temperature in 5 kOe for an alloy containing three magnetic phases.

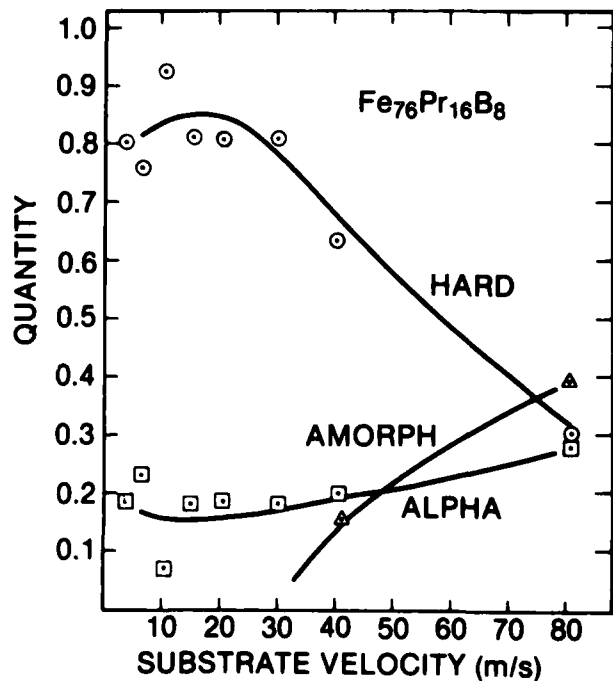


Figure 6. Relative amounts of phases as a function of substrate velocity.

## Identification of the hard phase

Figure 7 shows a transmission electron micrograph of the structure of a  $\text{Fe}_{76}\text{Pr}_{16}\text{B}_8$  ribbon solidified at 6 m/s. The major equiaxed grains, about 500 nm in diameter, have a Fe/Pr ratio of about 84/16, as shown by X-ray spectroscopy. The material between the grains is much richer in Pr, about  $\text{FePr}_3$ . Electron diffraction patterns from the major grains were consistent with the structure of  $\text{Fe}_{20}\text{Gd}_3\text{C}$  as reported in reference 25, with  $a = 8.81 \text{ \AA}$  and  $c = 11.78 \text{ \AA}$ . It appears that the hard phase is  $\text{Fe}_{20}\text{Pr}_3\text{B}$ , as was also indicated by Hadjipanayis et al.<sup>24</sup> This is reasonably consistent with the composition indicated by X-ray spectroscopy.

X-ray diffraction patterns generally showed many lines, a number of which could be indexed to the  $\text{Fe}_{20}\text{Pr}_3\text{B}$  phase, as well as on  $\alpha$ -Fe based phase. The most rapidly solidified samples showed a broad amorphous background peak.

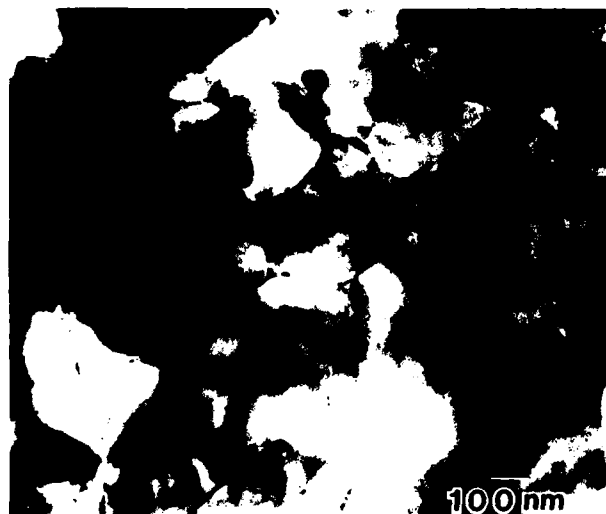


Figure 7. Transmission electron micrograph of  $\text{Fe}_{76}\text{Pr}_{16}\text{B}_5\text{Si}_3$  melt-spun at a substrate velocity of 6 m/s.

## Effects of annealing

Samples quenched at various rates were annealed at various temperatures. Then their magnetization-T curves and room-T hysteresis loops were measured as before. The results of a series of anneals on high-speed low- $H_{ci}$  material are summarized in Figure 8. When annealed at  $645^\circ\text{C}$ , the amorphous phase decomposes to a mixture of hard phase and  $\alpha$ . Annealing at  $750^\circ\text{C}$  for a short time produces more hard phase and less  $\alpha$ , but prolonged annealing at

that temperature increases the amount of  $\alpha$  relative to the amount of hard phase and drastically reduces  $H_{ci}$ . The hysteresis loops are shown to illustrate the correspondence of their shapes to the relative quantities of the phases given by the M-T curves.

When materials that were initially hard because of a slower quench rate were annealed, they became softer as the relative amount of hard phase decreased and  $\alpha$  increased. This is shown by the behavior of  $\text{Fe}_{74}\text{Pr}_{18}\text{B}_5\text{Si}_3$  cast at 13 m/s, which had a coercive force of 20.7 kOe as prepared. In this condition, the relative amounts of hard phase and  $\alpha$  were 0.84 and 0.16. After annealing at  $600^\circ\text{C}$  for 45 minutes, the loop was definitely 2-phase,  $H_{ci}$  was 1120 Oe, and the relative amounts were 0.46 and 0.54. Annealing the optimum- $H_{ci}$  structure reduces the amount of hard phase and produces more  $\alpha$ . The remaining hard phase seems less hard. However, whatever changes it is undergoing have little effect on its Curie temperature.

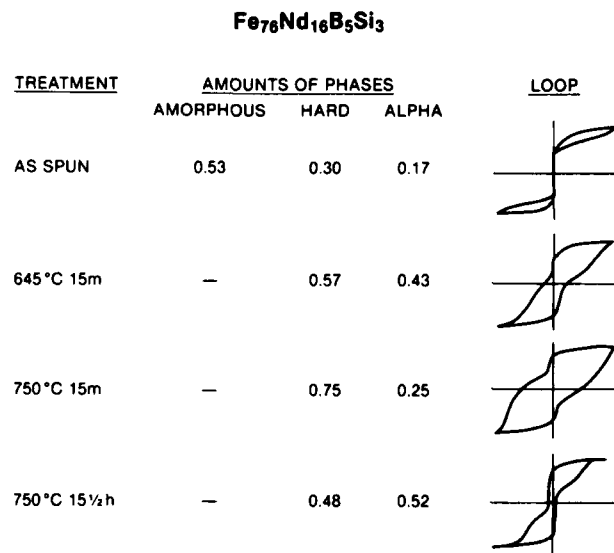


Figure 8. Relative amounts of phases and appearance of hysteresis loops in  $\text{Fe}_{76}\text{Nd}_{16}\text{B}_5\text{Si}_3$  after various treatments.

Thus, considerable amounts of the hard phase can be directly produced by quenching at the optimum rate. It can also be formed from the amorphous phase by short excursions to high temperatures, but longer anneals cause it to decompose, forming more  $\alpha$  phase. At low temperatures, the amorphous phase transforms to  $\alpha$ . Sometimes this can be observed during M-T runs at temperatures as low as  $400^\circ\text{C}$ .

## Etching experiments

The  $H_{ci}$  of a ribbon, either optimally quenched or rapidly quenched and annealed, inevitably varies through its thickness, since the quenching rate is greatest at the wheel and least on the free surface. This was illustrated in an experiment on samples of  $Fe_{76}Pr_{16}B_8$  shown in Figure 9. Two samples were solidified at 6 m/s. This is below the optimum rate, so  $H_{ci}$  should be greatest at the wheel surface. One sample was thinned by etching from the wheel side and the other from the free side. The  $H_{ci}$  of the first decreased with successive etches until it was less than half the original value; the second increased until  $H_{ci}$  had more than doubled. The same experiment was performed on samples solidified at 40 m/s, above the optimum rate, and the effect of etching was just the opposite.

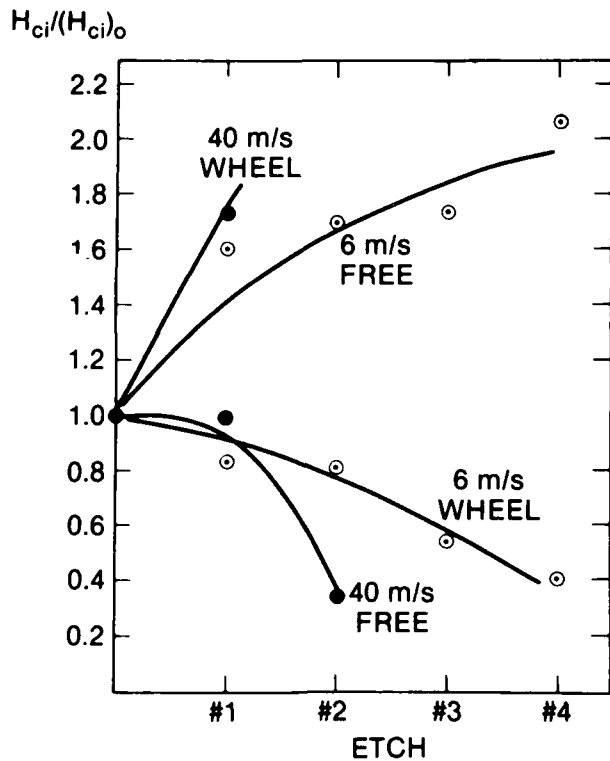


Figure 9. Change in  $H_{ci}$  resulting from etching different surfaces of  $Fe_{76}Pr_{16}B_8$  melt-spun at different speeds.

## Practical considerations

These iron-based light-rare-earth alloys have  $4\pi M_r$  values in the range of 10-15 kG. If such materials were near full density and the remanence

were nearly equal to the saturation, they could have energy products of 30-50 MGOe at the coercive force levels that have been attained. This would require single-crystal particles that could be aligned by a field and then densified by something like a liquid-phase sintering process, as with  $Co_5Sm$ . Perhaps more importantly, the potential for energy products of 10-20 MGOe with high resistance to demagnetization in materials of moderate cost seems very high, with less stringent requirements on processing. Perhaps the hard phase can be prepared in a more straightforward way than by melt-spinning.

The coercivity decreases rapidly with temperature, as shown in Figure 10. Although this seems to suggest that  $K$  of the hard phase decreases rapidly, it should be remembered that the plot really shows the temperature dependence of the reversal mechanism, i.e. of the effectiveness of reversal nuclei or of pinning sites.

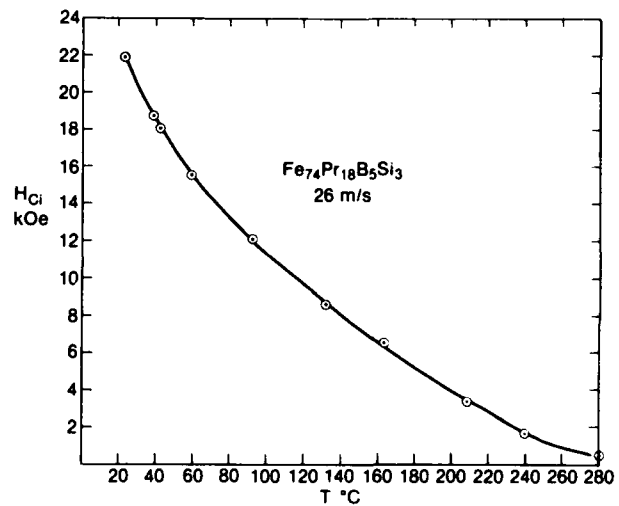


Figure 10.  $H_{ci}$  of  $Fe_{74}Pr_{18}B_5Si_3$  melt-spun at 26 m/s as a function of temperature.

The properties of different samples from the same run may be far from uniform. An extreme example is shown in Figure 11. Here the as-cast amorphous ribbons showed substantial variations in thickness, and therefore cooling rate, within a run. Sections of 1-mm wide ribbon a few mm long were taken from as-quenched ribbons of two different Tb alloys. These sections were selected to show a range of thicknesses. They were then annealed together at 650°C for 15

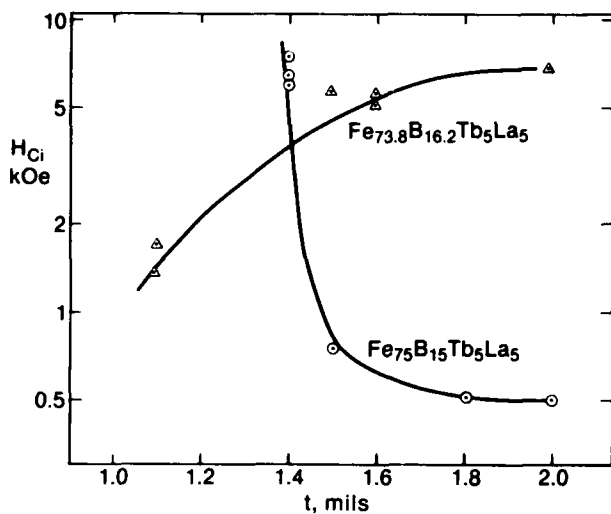


Figure 11.  $H_{ci}$  of two melt-spun Tb alloys annealed 15 minutes at 600°C at a function of initial thickness.

minutes. The thickness dependence of the resulting  $H_{ci}$  is striking not only in its magnitude but in the fact that in the two alloys it goes in opposite ways.

Finely divided rare-earth alloys are prone to oxidation. The  $H_{ci}$  of  $Co_5Sm$  powders decreases rapidly with time as surface nuclei are formed by oxidation of Sm, necessitating either a closed-pore structure produced by liquid-phase sintering or a pinning-controlled reversal process, as in the Cu-modified alloys, that is independent of surface nuclei. These considerations will certainly apply in a general way to the present iron-based alloys.

#### ACKNOWLEDGMENTS

Much of the experimental work on the iron-based rare earth alloys described here was done by R. A. Overfelt of the GE Small A. C. Motor Department. Thanks go to E. A. Hall and J. A. Sutliff for the electron microscopy and X-ray spectrometry, N. Marotta for DSC and TGA measurements, D. N. Wemple for experimental assistance, and J. D. Livingston for helpful discussions.

This work was partially supported by the Office of Naval Research.

#### REFERENCES

1. T. Egami, P. J. Flanders, and C. D. Graham, Jr., AIP Conf. Proc. **24**, 697 (1975).
2. F. E. Luborsky, J. J. Becker, and R. O. McCary, IEEE Trans. *MAG-11*, 1644 (1975).
3. F. E. Luborsky, Mat. Sci. and Eng. **28**, 139 (1977).

4. R. Hasegawa, R. C. O'Handley, and L. I. Mendelsohn, AIP Conf. Proc. **34**, 298 (1976).
5. U. Koster and U. Herold, "Glassy Metals," eds. H. J. Guntherodt and H. Beck, p. 225, Springer-Verlag, Heidelberg (1981).
6. M. Takahashi and M. Koshimura, Japan. J. Appl. Phys. **16**, 1711, 2269 (1977); M. Takahashi, C. O. Kim, M. Koshimura, and T. Suzuki, Japan, J. Appl. Phys. **17**, 1911 (1978).
7. M. Takahashi, T. Miyazaki, F. Ono, and K. Takakura, J. Japan Inst. Metals **40**, 1192 (1976).
8. A. A. Glazer, A. P. Potapov, V. V. Serikov, R. I. Tagirov, Y. I. Teytel, G. M. Makarova, and N. M. Kleynerman, Fiz. Met. metalloved. **48**, 1165 (1979); Phys. Met. Metall. **48**, 33 (1979).
9. J. C. Swartz, J. J. Haugh, R. F. Krause, and R. Kossowski, J. Appl. Phys. **52**, 1908 (1981).
10. S. F. H. Parker, P. J. Grundy, G. A. Jones, and R. S. Tebble, J. Appl. Phys. **53**, 7840 (1982).
11. V. R. V. Ramanan, J. Marti, and J. Macur, J. Appl. Phys. **52**, 1874 (1981).
12. A. R. Bhatti, P. J. Grundy, G. A. Jones, D. A. Scarsbrook, and R. S. Tebble, IEEE Trans. *MAG-16*, 1437 (1980).
13. J. J. Becker, IEEE Trans. *MAG-19*, 2033 (1983).
14. T. Jagielinski, IEEE Trans. *MAG-19*, 1925 (1983).
15. T. Mizoguchi, K. Yamauchi, and H. Miyajima, Proc. Intern. Conf. on Magnetism, Moscow, August 1973, vol. II, Nauka, Moscow (1974).
16. C. P. Chou and D. Turnbull, J. Non-Cryst. Solids **17**, 169 (1975).
17. L. E. Tanner and R. Ray, Scripta Met. **14**, 657 (1980).
18. J. L. Walter, S. F. Bartram, and I. Mella, Mat. Sci. and Eng. **36**, 193 (1978).
19. A. E. Clark, Appl. Phys. Lett. **23**, 642 (1973).
20. N. C. Koon and B. N. Das, Appl. Phys. Lett. **39**, 840 (1981).
21. J. J. Becker, IEEE Trans. *MAG-18*, 1451 (1982).
22. J. J. Croat, IEEE Trans. *MAG-18*, 1442 (1982).
23. G. C. Hadjipanayis, R. C. Hazelton, K. Lawless, and D. J. Sellmyer, IEEE Intermag Conference, April 5-8, 1983; to be published, IEEE Trans. on Magnetics.
24. G. C. Hadjipanayis, R. C. Hazelton, and K. R. Lawless, Appl. Phys. Lett. **43**, 797 (1983).
25. H. H. Stadelmaier and H. K. Park, Z. Metallk. **72**, 417 (1981).

J. J. Becker

**RAPIDLY QUENCHED METALS  
FOR PERMANENT MAGNET MATERIALS**

Report No. 84CRD094  
May 1984

GENERAL ELECTRIC COMPANY  
CORPORATE RESEARCH AND DEVELOPMENT  
P.O. BOX 8, SCHENECTADY, N.Y. 12301

**GENERAL ELECTRIC**

**APPENDIX B**  
**84CRD089**

# CRD

---

Corporate Research and Development

---

Schenectady, New York

---

**THERMAL EFFECTS OF  
MODERATE SUBSTITUTIONS  
OF COBALT FOR IRON  
IN  $\text{Fe}_{76}\text{Pr}_{16}\text{B}_8$**

by

**R. A. Overfelt\* and J. J. Becker  
Metallurgy Laboratory**

**Report No. 84CRD089**

**May 1984**

\*Vanderbilt University

---

Technical Information Series

---

Class 1

---

**GENERAL  ELECTRIC**

# TECHNICAL INFORMATION SERIES

<small>AUTHOR</small> Overfelt, R A* Becker, J J	<small>SUBJECT</small> permanent magnetic materials	<small>NO.</small> 84CRD089
		<small>DATE</small> May 1984
<small>TITLE</small> Thermal Effects of Moderate Substitutions of Cobalt for Iron in $Fe_{76}Pr_{16}B_8$		<small>GE CLASS</small> 1
		<small>NO. PAGES</small> 3
<small>ORIGINATING COMPONENT</small> Metallurgy Laboratory	<small>CORPORATE RESEARCH AND DEVELOPMENT</small> SCHENECTADY, N. Y.	
<small>SUMMARY</small>  We have explored the thermal effects of moderate substitutions of cobalt for iron in rapidly solidified, microcrystalline alloys of composition $(Fe_{100-x}Co_x)_{76}Pr_{16}B_8$ where $x = 0, 5, 10, 20,$ and $30$ . The maximum intrinsic coercivities were about 20 kOe and the saturation magnetizations were about 88 emu/g, both independent of cobalt content. A significant improvement in the Curie temperature of the hard phase is obtained with increasing cobalt content. A similar improvement in the reversible and irreversible temperature behavior is also observed as the cobalt content is increased.		
<small>KEY WORDS</small> permanent magnet, magnetic materials, rapid solidification, Curie temperature		

\*Vanderbilt University

INFORMATION PREPARED FOR \_\_\_\_\_

Additional Hard or Microfiche Copies  
Available from

Technical Information Exchange  
Bldg. 5 Room 321, Schenectady, N.Y. 12345

# THERMAL EFFECTS OF MODERATE SUBSTITUTIONS OF COBALT FOR IRON IN $\text{Fe}_{76}\text{Pr}_{16}\text{B}_8$

R. A. Overfelt\* and J. J. Becker

Recently there has been a considerable amount of work in iron-rare earth-boron materials for permanent magnets. Several researchers including Hadjipanayis, Hazelton, and Lawless,<sup>1</sup> Sellmyer and Hadjipanayis,<sup>2</sup> Koon,<sup>3</sup> Croat, Herbst, Lee, and Pinkerton,<sup>4</sup> and Becker<sup>5</sup> utilized rapid solidification in alloys of iron, neodymium or praseodymium, and boron to achieve very large  $H_{ci}$  and large energy products. Sagawa et al<sup>6</sup> succeeded within this same alloy system in obtaining  $(BH)_{max} = 35\text{-}40$  MGOe by traditional powder techniques. The high- $H_{ci}$  phase has been identified as a tetragonal phase with  $a = 0.0881$  nm and  $c = 1.178$  nm<sup>1,2,3,4,5,6</sup> with a Curie temperature of around 300°C, which presents obvious disadvantages in some applications.

This letter reports the beneficial effects on  $T_c$  of moderate amounts of cobalt in the composition  $(\text{Fe}_{100-x}\text{Co}_x)_{76}\text{Pr}_{16}\text{B}_8$  where  $x = 5, 10, 20,$  and  $30$ . Maximum  $H_{ci}$  of 20 kOe were observed in all of the alloys solidified at 20-30 m/s. The saturation magnetizations were about 88 emu/g independent of cobalt content.

Alloys of nominal composition were made by melting commercially available constituents in alumina or zirconia crucibles under an atmosphere of argon. Pieces from these ingots were induction melted in a silica crucible and then ejected by about 20 psi argon pressure through a 0.050 inch orifice onto a rapidly rotating copper wheel. The distance between the crucible and the copper wheel was approximately 0.5 inch. All melt spinning was done under argon atmosphere.

The magnetic hysteresis loops were measured with a vibrating sample magnetometer in a 12 inch electromagnet. All of the magnetization versus temperature runs were done in the VSM using a 1 inch diameter tin oxide coated resistance furnace

heating at about 50°/min. Samples were saturated by heating above  $T_c$  of the respective hard phase in a 5 kOe field. The magnetization was then locked in by cooling in the field.

Figure 1 shows a typical hysteresis loop. The very high coercivities prevented saturation with the 20 kOe magnetic fields possible with the 12 inch electromagnet. Thus, the actual loops normally obtained were only minor loops vertically displaced as shown by the solid curve of Figure 1. The dashed curve shows the rest of the anticipated full hysteresis loop. These measurements were always made after the sample had been saturated as described above. The Curie temperature of the hard phase was defined as the inflection point in the 5 kOe  $M(T)$  curve. The dip in magnetization at remanence was seen often and indicates a soft component.<sup>7</sup>

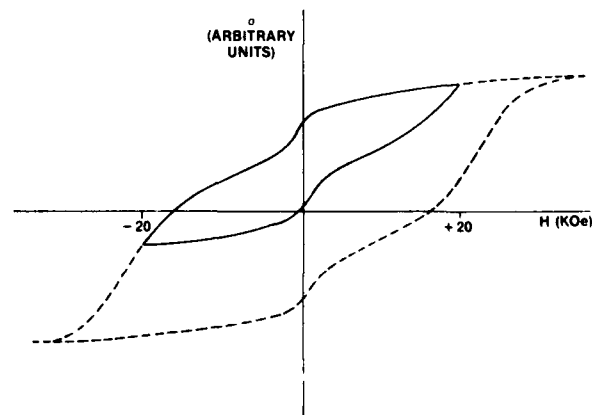


Figure 1. Displaced minor hysteresis loop resulting from cooling in a 5 kOe field. Full anticipated hysteresis loop is shown by the dashed curve.  $\text{Fe}_{76}\text{Pr}_{16}\text{B}_8$  solidified at 20 m/s.

\*Vanderbilt University

The samples were small pieces of rapidly solidified ribbons weighing approximately 15 mg. The samples' self-demagnetizing fields have not been corrected for but should influence the data relatively little due to the hard phase's very large anisotropy fields. Figure 2 shows normalized magnetization versus temperature data for these alloys in a 5 kOe field and shows how the Curie temperature of the hard phase is affected by cobalt content. Some magnetization, presumably due to  $\alpha$ -Fe,<sup>5</sup> remains at higher temperatures. These curves should closely reflect the reversible behavior of the remanences of bulk magnets, since under reversible conditions the domain structure at remanence does not change. The Curie temperature of the hard phase is seen to increase from 285°C for  $x = 0$  to 350, 440, and 505°C for  $x = 10$ , 20, and 30 respectively. Note that  $T_c$  is raised by more than 15°C for each percent of cobalt referred to total alloy composition. The temperature coefficient of the magnetization is seen to improve from  $-0.14\%/^{\circ}\text{C}$  for  $x = 0$  to  $-0.05\%/^{\circ}\text{C}$  for  $x = 30$ .

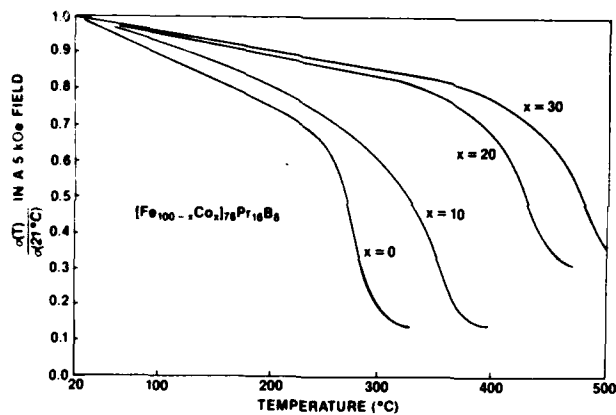


Figure 2. Magnetization versus temperature for alloys with various cobalt contents. Samples solidified at 20-30 m/s.

Figure 3 shows the decrease in room-temperature remanence after momentary exposure to an elevated temperature in zero field. Figure 4 shows the decrease in the field required, at room temperature, to reduce the magnetization from the new remanence to zero. Again, corrections for the samples' self-demagnetizing fields have not been applied. The losses shown in Figures 3 and 4 are irreversible, that is, they are losses that are only regained on remagnetization. In Figure 3, the irreversible changes in remanence over the temperature range 20–100°C

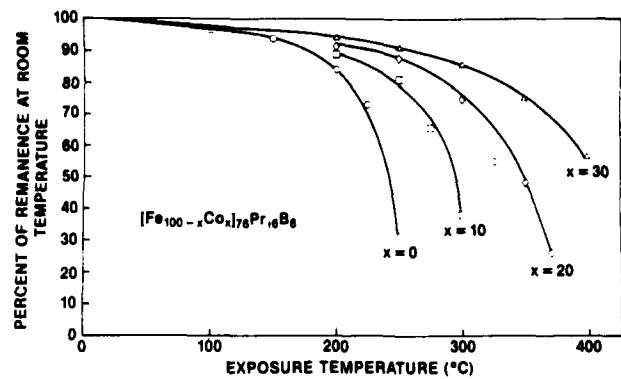


Figure 3. Percent of remanence after momentary exposure to indicated elevated temperature in zero applied field as a function of cobalt content.

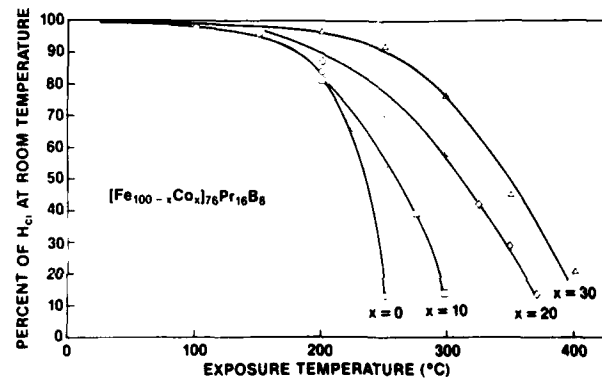


Figure 4. Percent of intrinsic coercivity after momentary exposure to indicated elevated temperature in zero applied field as a function of cobalt content.

improve from  $-0.06\%/^{\circ}\text{C}$  for  $x = 0$  to  $-0.03\%/^{\circ}\text{C}$  for  $x = 30$ . The behavior of the coercive force shown in Figure 4 is similar to that of the remanence in Figure 3. In both cases the stability to temperature exposures of more than about 200°C is greatly improved by the addition of cobalt.

In summary, moderate substitutions of cobalt for iron will significantly improve the high temperature behavior of these new alloys. Although these data were taken on small pieces of rapidly solidified ribbons, the beneficial effects due to cobalt substitutions in these samples should approximate the behavior of bulk magnets of the same compositions.

## ACKNOWLEDGEMENTS

The authors are grateful for the technical assistance of W. Moore, N. Marotta, and E. Hall. The enthusiastic support of L. A. Johnson and J. F. Larson are also appreciated.

This work was partially supported by the Office of Naval Research.

## REFERENCES

1. G. C. Hadjipanayis, R. C. Hazelton, and K. R. Lawless, *J. Appl. Phys.* *55*, 2073 (1984).
2. D. J. Sellmyer and G. C. Hadjipanayis, *J. Appl. Phys.* *55*, 2088 (1984).
3. N. C. Koon, *J. Appl. Phys.* *55*, 2063 (1984).
4. J. J. Croat, J. F. Herbst, R. W. Lee, and F. E. Pinkerton, *J. Appl. Phys.* *55*, 2078 (1984).
5. J. J. Becker, *J. Appl. Phys.* *55*, 2067 (1984).
6. M. Sagawa, S. Fujimura, M. Togawa, H. Yamamoto, and Y. Matsuura, *J. Appl. Phys.* *55*, 2083 (1984).
7. J. J. Becker, *IEEE Trans. Magn.*, *MAG-18*, 1451 (1982).

R. A. Overfelt\*  
J. J. Becker

THERMAL EFFECTS OF  
SUBSTITUTIONS OF COBALT FOR IRON  
IN  $\text{Fe}_{76}\text{Pr}_{16}\text{B}_8$

Report No. 84CRD089  
May 1984

GENERAL ELECTRIC COMPANY  
CORPORATE RESEARCH AND DEVELOPMENT  
P.O. BOX 8, SCHENECTADY, N.Y. 12301

**GENERAL ELECTRIC**

**APPENDIX C**  
**84CRD095**

# CRD

---

Corporate Research and Development

---

Schenectady, New York

---

**SURFACE EFFECTS ON THE COERCIVE FORCE  
OF RAPIDLY SOLIDIFIED Fe-Pr-B ALLOYS**

by  
J.J. Becker and R.A. Overfelt\*  
Metallurgy Laboratory

Report No. 84CRD095

May 1984

\*Vanderbilt University

---

Technical Information Series

---

Class 1

---

GENERAL  ELECTRIC



# SURFACE EFFECTS ON THE COERCIVE FORCE OF RAPIDLY SOLIDIFIED Fe-Pr-B ALLOYS

J. J. Becker and R. A. Overfelt

## INTRODUCTION

There has been a great deal of recent interest in the permanent magnet properties of rapidly solidified alloys containing about 75 atomic percent Fe, 15 percent Pr or Nd, and 10 percent B, both in the form of rapidly quenched ribbons [1-5] and as sintered powders [6]. Melt-spun ribbons can be either rapidly quenched and annealed [1-3] or quenched at an intermediate rate to produce high  $H_{ci}$  directly [4,5]. In the melt spinning process, in which material is solidified on a rapidly rotating wheel into ribbon form, the quenching rate would be expected to be greatest at the wheel surface and least at the free surface. Thus the micro structure will inevitably vary through the thickness of the material, and so also will the coercivity  $H_{ci}$ , with its extreme structure-sensitivity.

## EXPERIMENTAL

We prepared each ribbon of  $Fe_{76}Pr_{16}B_8$  by melting the alloy in a quartz tube having an 0.13 cm opening in the bottom and ejecting the molten metal with argon on to a rotating copper wheel 7.6 cm in diameter from a distance of about 1 cm. The surface speed of the wheel varied from 4 to 80 m/s. The magnetic properties were measured in a vibrating-sample magnetometer using a sample consisting of a single piece of ribbon usually less than 1 cm long. Etching was done on individual samples using 30%  $HNO_3$ .

## RESULTS AND DISCUSSION

Figures 1 and 2 show, at two different wheel speeds, that the grain size does indeed increase from wheel surface to free surface.

A plot of the  $H_{ci}$  of ribbons solidified at various wheel speeds shows the relationship in Figure 3. The low  $H_{ci}$  at high speeds is associated with the presence of amorphous phase, while at low speeds the grain size is large. At an intermediate wheel surface speed of 20 or 30 m/s the  $H_{ci}$  is greatest. Each point in Figure 3 represents an average of at least three samples. While the trend in Figure 3 is quite unmistakable, there can be considerable variation from one run to another and especially among

different short samples of ribbon from the same run. It is very generally observed in melt-spun ribbons that air pockets occur on a substantial fraction of the wheel surface of the ribbon, resulting in a pattern of local regions of lower cooling rate and causing irregular cross-sections [7]. The present materials are certainly no exception. Sometimes nodules of large-grain material appear at a pocket; Figure 4 shows an especially prominent example. In Figure 5, the large-grain structure can be seen to go all the way through to the wheel surface. These kinds of things occur at all wheel speeds and cause a scatter in  $H_{ci}$  when it is measured in very short lengths of ribbon. Thus each point in Figure 3 might have a total spread of something like a factor of two.

The variation in  $H_{ci}$  through the thickness was revealed by preferentially etching either the wheel surface or the free surface of samples of  $Fe_{76}Pr_{16}B_8$  that had been solidified at various rates, and whose average as-quenched properties are shown in Figure 3. Samples solidified at 40 m/s, which was too fast, should have higher  $H_{ci}$  at the free surface, which was solidified less rapidly and thus at closer to the optimum rate. Etching the free surface should then decrease  $H_{ci}$ , while etching the wheel surface should increase it. Figure 6 shows that this is what happened when the experiment was carried out. The  $H_{ci}$  dropped by 65% after the free surface was etched. For a ribbon solidified at 8 m/s, the material nearest the wheel should have the highest  $H_{ci}$ , and etching should have the opposite effect on  $H_{ci}$ . Again, Figure 6 shows that this is what happened. A 6 m/s ribbon showed the same behavior as the 8 m/s but still more strongly, as it should. For a solidification rate such that the  $H_{ci}$  of the total ribbon was a maximum, one might expect that the material in the center would have the highest  $H_{ci}$  and that therefore etching either surface would tend to produce a rather small increase in  $H_{ci}$ . However, the 20 m/s sample shown in Figure 3 behaved more like a somewhat-faster-than-optimum ribbon. Examination of this sample revealed some air pockets at the wheel surface, associated with some larger grains of presumably lower coercivity. Etching this surface should then raise  $H_{ci}$ , as indeed it did.

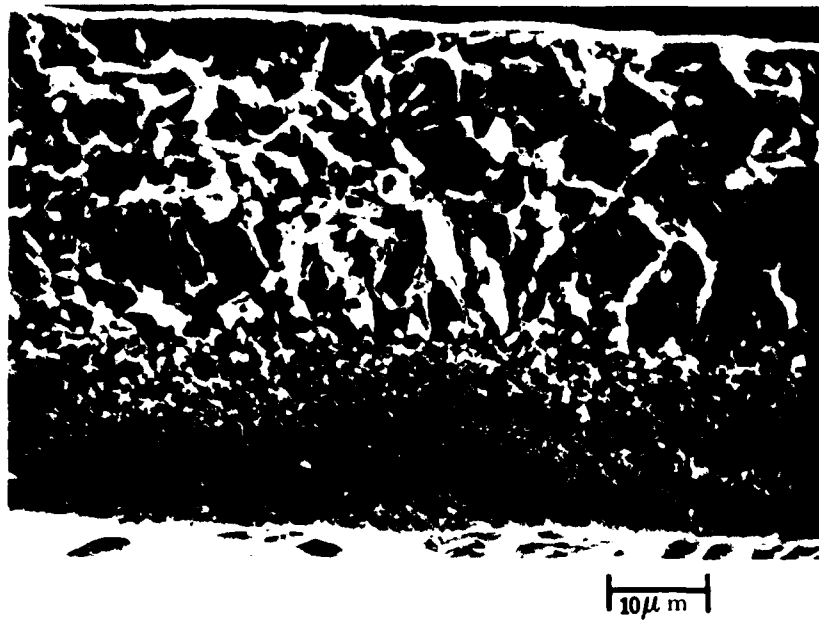


Figure 1. Scanning electron micrograph of fracture cross section of Fe<sub>76</sub>Pr<sub>16</sub>B<sub>8</sub> ribbon solidified at 4 m/s

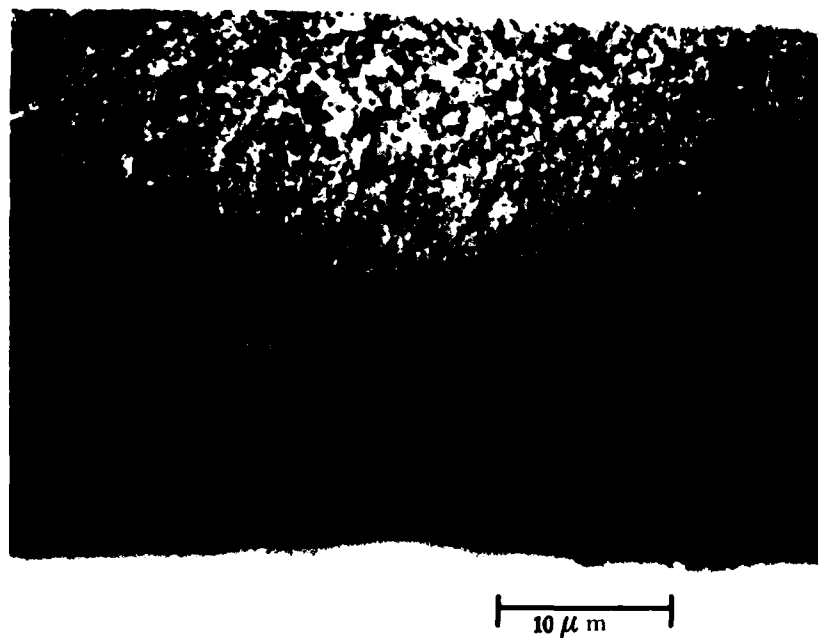


Figure 2. Scanning electron micrograph of fracture cross section of Fe<sub>76</sub>Pr<sub>16</sub>B<sub>8</sub> ribbon solidified at 20 m/s

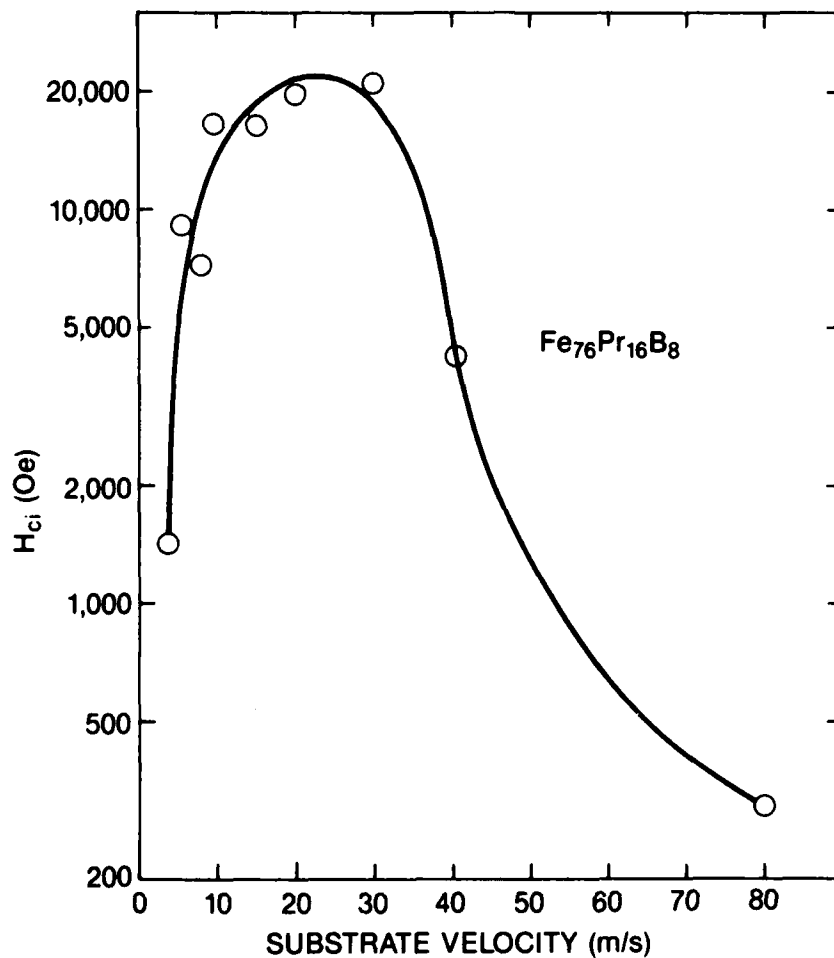


Figure 3. Dependence of coercivity  $H_{ci}$  on substrate velocity for  $Fe_{76}Pr_{16}B_8$  ribbons

The trends in coercive force and etching behavior shown in these experiments seem quite clear. The considerable variability among individual samples illustrates that at least under these conditions there is room for substantial improvement of the average properties through better processing uniformity. If permanent magnets are to be made from rapidly solidified materials that are compacted in some way,

it appears that considerations such as these will have an important bearing on the properties that may be attainable.

#### ACKNOWLEDGEMENT

This work was supported in part by the Office of Naval Research.

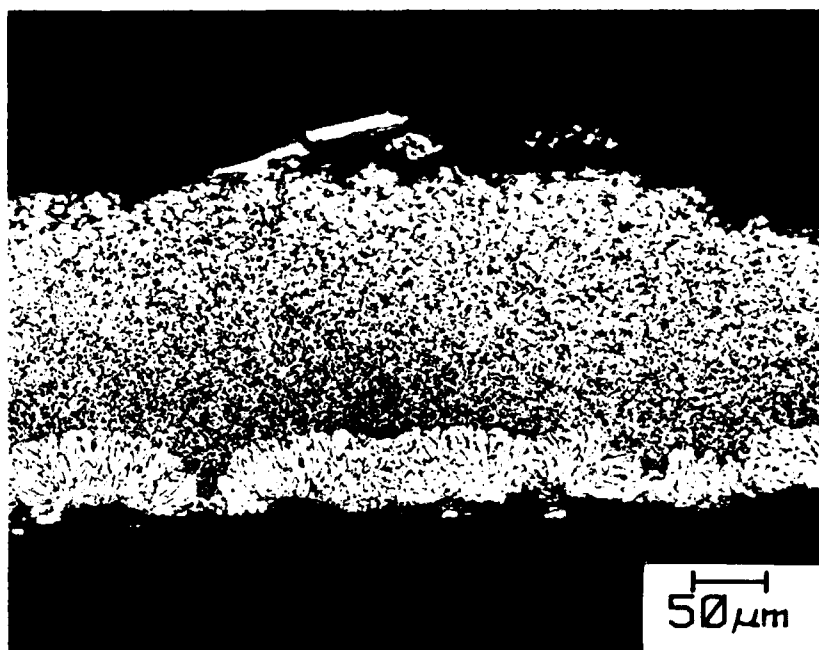


Figure 4. Optical micrograph of cross section of Fe<sub>76</sub>Pr<sub>16</sub>B<sub>8</sub> ribbon solidified at 6 m/s



Figure 5. Scanning electron micrograph of fracture cross section of Fe<sub>76</sub>Pr<sub>16</sub>B<sub>8</sub> ribbon solidified at 30 m/s

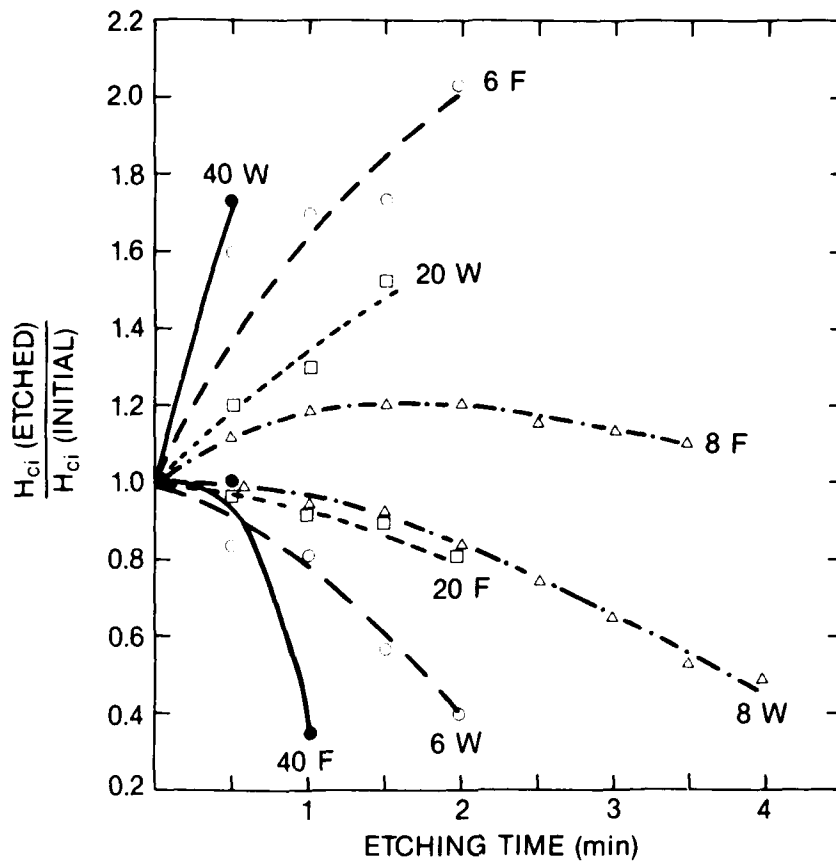


Figure 6. Etching behavior of  $\text{Fe}_{76}\text{Pr}_{16}\text{B}_8$  ribbons. Numbers within plot are solidification rate in m/s

F = free surface etched  
W = wheel surface etched

#### REFERENCES

1. G. C. Hadjipanayis, R. C. Hazelton, and K. B. Lawless, *J. Appl. Phys.* **55**, 2073 (1984).
2. D. J. Sellmyer, A. Ahmed, G. Muench, and G. Hadjipanayis, *J. Appl. Phys.* **55**, 2088 (1984).
3. N. C. Koon and B. N. Das, *J. Appl. Phys.* **55**, 2063 (1984).
4. J. J. Croat, J. F. Herbst, R. W. Lee and F. E. Pinkerton, *J. Appl. Phys.* **55**, 2078 (1984).
5. J. J. Becker, *J. Appl. Phys.* **55**, 2067 (1984).
6. M. Sagawa, S. Fujimura, M. Togawa, H. Yamamoto, and Y. Matsuura, *J. Appl. Phys.* **55**, 2083 (1984).
7. S.-C. Huang and H. C. Fiedler, *Met Trans.* **12A**, 1107 (1981).

J.J. Becker SURFACE EFFECTS ON THE COERCIVE FORCE Report No. 84CRD095  
R.A. Overfelt OF RAPIDLY SOLIDIFIED Fe-Pr-B ALLOYS May 1984

GENERAL ELECTRIC COMPANY  
CORPORATE RESEARCH AND DEVELOPMENT  
P.O. BOX 8, SCHENECTADY, N.Y. 12301

**GENERAL ELECTRIC**

**END**

**FILMED**

7-85

**DTIC**